IEEE Access
Multidisciplinary ⋮ Rapid Review ⋮ Open Access Journal

Received 22 October 2023, accepted 30 November 2023, date of publication 12 December 2023,
date of current version 19 December 2023.

Digital Object Identifier 10.1109/ACCESS.2023.3341498

RESEARCH ARTICLE

Fuzzy Dynamic Modeling for Accurate Control of Uncertain Mechanical Systems

CHENDI SHI[1] **AND BAO LIU**[2]
[1]Department of Rural Revitalization Education, Jilin Engineering Vocational College, Siping 136001, China
[2]Department of Management, Jilin Engineering Vocational College, Siping 136001, China

Corresponding author: Chendi Shi (shichendi1997@163.com)

ABSTRACT Mechanical systems become more complex, achieving precise control becomes increasingly challenging due to uncertainty. This study presents a fuzzy dynamics-based strategy for precise control of uncertain mechanical systems and investigates the use of robust control theory to assess system performance and stability under constraints. Fuzzy theory enables uncertainties to be addressed, resulting in a more precise description of system behaviour. The study findings demonstrate that utilising the constraint invariant dynamics analysis method led to a decrease in control input amplitude, resulting in an average total input U reduction of approximately 60 volts and improving system stability. The constraint invariant dynamics analysis method led to an average reduction of 40 volts in u1 amplitude and an average position error of 1 mm under motor control. The experimentation undertaken on the permanent magnet synchronous motor angular trajectory exhibits that each test was successful in following the anticipated path. The average angular discrepancies between experiments A, B, C, and D were 0.5, 1, 0.3, and 0.8 degrees respectively. The experimental trajectories for A and B occasionally surpassed the upper limit, while C and D remained consistently within the upper and lower bounds. The implementation of the state-dependent control strategy resulted in a 10% reduction in standard deviation of current fluctuation on average, further enhancing the stability and efficiency of the motor system. The research results are expected to provide more stable and efficient control solutions for a wide range of industrial and engineering applications, thereby making a positive contribution to sustainable development and technological progress in society.

INDEX TERMS Control strategies, uncertain mechanical systems, CIDA method, fuzzy dynamics, HORC control.

I. INTRODUCTION

Achieving precise control over mechanical systems has posed a significant challenge in engineering control. A variety of uncertainties, including external perturbations, sensor errors, friction, and component manufacturing errors, typically impact mechanical systems [1]. Traditional methods have obvious shortcomings in dealing with the uncertainty of mechanical systems. First of all, traditional accurate models often cannot accurately describe various uncertain factors in the system, such as friction, external disturbances, etc. Secondly, traditional control methods are usually designed based on accurate dynamic models of the system. However, parameters in the actual system are often affected by various factors and change, resulting in inaccurate models and thus affecting control performance. Unlike the conventional deterministic dynamics model, the Fuzzy dynamics (FD) model incorporates fuzzy logic and fuzzy set theory to better cope with uncertain elements and attain PC in mechanical systems [2]. The novelty of this study lies in applying FD model design to Uncertain Mechanical Systems (UMS) and presenting a new approach to constructing these models. The proposed methodology combines fuzzy logic, hybrid systems theory and modern control techniques to develop an efficient and robust control framework, capable of achieving precise control of mechanical systems in complex and uncertain environments. By combining finite difference modelling with established control techniques, the study aims to offer a flexible and dependable control solution for the engineering sector. This will elevate the performance of UMS to new

The associate editor coordinating the review of this manuscript and approving it for publication was Ming Xu.

levels. Furthermore, the research focuses on incorporating fuzzy control (FC) and robust control to manage the system's intrinsic uncertainties and external disturbances. The fuzzy robust controller will be designed with a focus on optimising the affiliation function and control gain of the fuzzy set for the UMS's PC [3]. The research results are expected to provide new ideas and solutions for the control design of uncertain mechanical systems and promote research and applications in related fields.

The study consists of four parts, the first part summarises the control and FD models of UMS; the second part presents the FD-based PC strategy for UMS; the third part covers the FD modelling and control validation of UMS; and the fourth part concludes the full paper.

II. RELATED WORKS

PC of UMS is a research area involving the fields of mechanical engineering and control engineering, which has been studied by many experts. Cortez et al. found that mechanical systems with critical actuator, velocity and position constraints are essential for safety and mission execution, and they developed novel, robust control barrier functions for ensuring that the constraints of a sampled data system are satisfied in the presence of model uncertainty [4]. Yang et al. found that one of the main characteristics of underdriven systems is the lack of a sufficient number of control inputs, and proposed an analytical approach based on composite surfaces that rigorously proved the asymptotic stability of the system's equilibrium point [5]. Zhao et al. successfully address the challenges of asymmetric dead-zone nonlinearities and external perturbations by implementing vibration control and dead-zone compensation for uncertain spatial flexible riser systems. They achieve this through modelling the asymmetric dead-zone nonlinearities and representing them as required control inputs. Additionally, they introduce extra nonlinear input errors to account for uncertainties [6]. In order to deal with state-dependent uncertain systems and to consider randomly occurring replay attacks, DoS attacks, and spoofing attacks in a unified framework, Liu's team first proposed a multiple attack model, which uniformly takes randomly occurring replay attacks, DoS attacks, and spoofing attacks into account. And they used event triggering mechanism to reduce the communication frequency to save the limited resources [7]. Liu et al. addressed the problem of event-based security control for state-dependent uncertain systems under hybrid attacks by adopting an event-triggered scheme to reduce the communication frequency, and derived a sufficient condition for the exponential mean-square stability of state-dependent uncertain systems by using the Lyapunov-Krasocskii stability theory and the linear matrix inequality technique [8].

The goal of FD model design is to develop a mathematical model adapted to fuzzy, uncertain information that can better capture and describe the dynamic behaviour of real systems. Ji Wenqiang and other scholars, for the output feedback sliding mode control (SMC) problem for discrete-time uncertain nonlinear systems, adopt the Takagi-Sugeno fuzzy dynamic model to describe the system and incorporate sliding surfaces to construct the descriptive subsystem, and use the segmented quadratic Lyapunov function to obtain sufficient conditions for the asymptotic stability analysis of the sliding motion through a convex optimisation setup [9]. Huang et al. adopted a broad fuzzy neural network (BFNN) to construct Control strategies (CS) in response to the problem of how to use a broad learning system (BLS) to solve the problem of selecting a sufficient number of neural network units to approximate an unknown dynamical model and to take advantage of the broad learning system (BLS) to solve the neural network unit number selection problem [10]. Liang et al. addressed the problem of how to design the reference pitch and yaw angles in order to implement time-varying reference trajectories in kinematics. In order to enhance the robustness of the system, a fuzzy-based adaptive DSC scheme was used to adapt to the complex unknown factors [11]. Wang et al. and his group members introduced the fuzzy theory to the spatial co-location model for how to determine the subsets of spatial feature sets efficiently, and developed a reasonable metric by considering the fuzzy proximity between spatial instances, taking into account the issue of instance sharing and the similarity between different spatial features [12]. Hu et al. and his group members about the comprehensive assessment method of cloud manufacturing services, based on fuzzy comprehensive evaluation (FCE), used a combination of qualitative and quantitative methods. A comprehensive evaluation index system and a fuzzy trapezoidal affiliation function were established for a more comprehensive assessment of cloud manufacturing services [13].

In summary, many experts have researched for UMS and FD models, but the current model uncertainty will affect the control performance to a certain extent, the study proposes the design of FD model for PC of UMS to improve the model accuracy and performance, and it is expected to provide more powerful tools and methods for PC of UMS.

III. PC STRATEGY FOR FD-BASED UMS

This chapter focuses on CS in the presence of inequality constraints in a UMS and the relationship between constraint following and system stability, and analyses the stability of the system in an uncertain environment. Finally, it describes how to model uncertainties using fuzzy set theory and apply these models to CS.

A. CS FOR UMS WITH INEQUALITY CONSTRAINTS

In order to tightly control the amplitude of the control inputs, an improved robust controller design method is investigated. The core idea of this method is to use the principle of differential homogeneous transformation to redefine the originally unconstrained control input as a bounded function of auxiliary variables. This bounded function has a relatively simple selection and construction process, allowing the engineer to set the values of the control inputs according to the actual

needs, thus improving the flexibility and applicability of the system [14]. This approach is more general and provides a new paradigm for dealing with the input constraint problem in UMS, as shown in equation (1).

$$\dot{x}(t) = f(x(t), t) + B(x(t), t)\Phi(w(t), \sigma(t), t) + B(x(t), t)e(x(t), \sigma(t), t) \tag{1}$$

In equation (1), $t \in R$ denotes the time, $x(t) \in R^n$ denotes the state, $\sigma(t) \in \sum \subset R^p$ denotes the time-varying uncertain parameters, $w(t) \in R^m$ denotes the inputs, and the function $\sigma(\cdot)$ can be used to denote that Lebesgue is measurable and the value lies in the tight set $\sum \subset R^p$. If in the design situation, a boundary is required for the input, then $w(t) \in W$, where $W \to R^m$, $(m) = u$, $w = ^{-1}(u)$, can make $\Phi(w(t), \sigma(t), t) = \Phi(^{-1}(u(t)), \sigma(t), t) =: \hat{\varphi}(u(t), \sigma(t), t)$. So equation (1) can be rewritten as shown in equation (2).

$$\dot{x}(t) = f(x(t), t) + B(x(t), t)\hat{\varphi}(u(t), \sigma(t), t) + B(x(t), t)e(x(t), \sigma(t), t) \tag{2}$$

In equation (2), $u(t) \in R^m$ can be regarded as either a new controller or an auxiliary control. The control input limitation process based on inequality constraints needs to explicitly define the control input constraints of the UMS, and the designer needs to select an appropriate control function (usually denoted as $\hat{\varphi}$), which relates the control inputs to the system states or outputs, and the selection of the control function $\hat{\varphi}$ should take into account the dynamics of the system and the constraints to ensure that the selected function can play an effective role in the control of the system. The parameters in the control function $\hat{\varphi}$ (usually denoted as λ) allow the designer to specify the specific boundaries of the control inputs [15]. The setting of these parameters is critical as they will determine the effective range of the control inputs to vary within the constraints. In order to satisfy the inequality constraints on the control inputs, it is necessary to select appropriate auxiliary functions (often notated as $\hat{\gamma}$, $\hat{\Psi}$, $\hat{p}$, etc.). These functions should be selected taking into account the characteristics of the system to ensure that they are effective in limiting the control inputs to the range specified by the control function $\hat{\varphi}$ [16]. The flow of control input limitation based on inequality constraints is shown in Figure 1.

A flowchart of the Constraint-Invariant Dynamic Analysis (CIDA) method is presented in Figure 1. The improved control $u(t)$ is able to endow the UMS with the following performance characteristics, firstly, the system possesses consistently bounded performance, i.e., for any given $r > 0$, if the output of the system under the initial conditions is $\|x(t)\| \leq d(r)$, then there exists a positive number $d(r)$ associated with r, such that for all time points satisfying $t \geq t_0$, the output of the system remains within the range of $\|x(t)\| \leq d(r)$. Secondly, the system also exhibits consistent ultimately bounded performance, i.e., for any given $r > 0$, if the output of the system under the initial conditions is $\|x(t)\| \leq d(r)$, then there exist r-dependent positive numbers $d(r)$ and

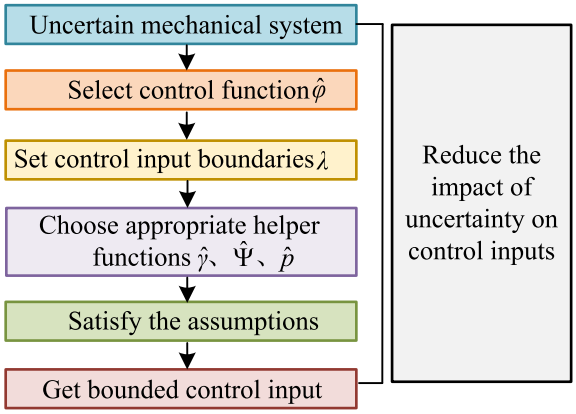

FIGURE 1. Control input restriction process based on inequality constraints.

$T(d(r), r)$ such that the output of the system, $\|x(t)\| \leq \bar{d}$ E, stays within the range of $d(r) > 0$, $T(\bar{d}(r), r) \geq 0$ for all the time points that satisfy $t \geq t_0 + T(d(r), r)$. The structure of the electrical throttle system designed by the study is shown in Figure 2.

Figure 2 shows the structure and composition of the electronic throttle system, which is divided into two parts: the electronic throttle mechanism and the electronic control unit (ECU). The electronic throttle mechanism is responsible for outputting the throttle angle, which is achieved through the synergistic action of gears, turntable 1, turntable 2 and service motor. At the same time, the ECU plays the central role of control, generating the required angle signal OD based on the throttle pedal signal and the actual angle signal OV from the throttle angle sensor, and transmitting it to the service motor [16]. This system possesses complex mechanical and electrical structures, which include mechanical mechanisms such as springs and gears as well as electromechanical structures such as motors.

$$I_t(t)K_{RD}K_{DP}\ddot{\theta}_v(t) = \frac{T_M(t)}{K_{VT}K_{TM}} + T_f(t) - \frac{T_s(t)}{K_{VT}} \tag{3}$$

In equation (3), the relationship between the proportional angle θ_v and the actual angle θ_α is shown in equation (4).

$$\theta_v(t) = K_{VT}\theta_\alpha(t) \tag{4}$$

The resistance torque and the load torque applied by the reset spring, the expression is shown in equation (5).

$$\begin{cases} T_s(t) = K_{s1}K_{DP}\theta_\alpha(t) + K_{s2} \\ T_f(t) = T_c(t) + T_v(t) \end{cases} \tag{5}$$

In equation (5), $T_v(t) = -fvK_{RD}K_{DP}\dot{\theta}_v(t)$, $T_c(t)$ denote the viscous friction moment and Coulomb friction moment, viscous friction moment is a kind of friction moment due to the viscous effect in liquid or gaseous medium; Coulomb friction moment is a kind of friction moment due to the effect of dry friction, which results in the relative motion between two surfaces being resisted when there is no lubricating medium between the two surfaces [17], [18].

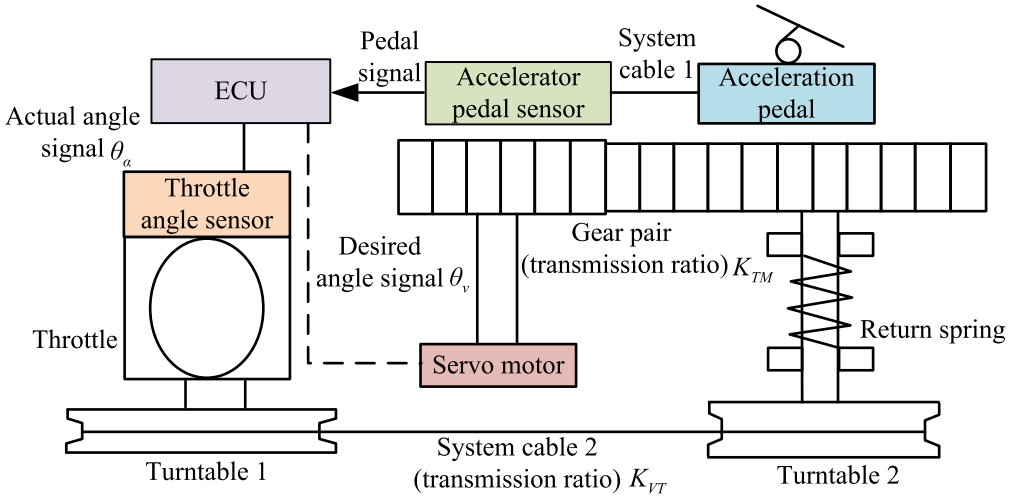

FIGURE 2. Electronic throttle system structure.

B. ANALYSIS OF THE ASSOCIATION BETWEEN CONSTRAINT FOLLOWING AND SYSTEM STABILITY BASED ON ROBUST CONTROL THEORY

In real nonlinear mechanical systems, uncertainties such as parameter uncertainties and external disturbances are usually present, and they often cannot be ignored because of their important impact on the dynamic performance of the system. For this consideration, the dynamics model of a constrained mechanical system with uncertain parameters is investigated. It is shown in equation (6).

$$\hat{M}(y(t), \delta(t)\ddot{y}(t) = \hat{Q}(y(t), \delta(t), t) + u(t) \tag{6}$$

In equation (6), $t \in R$, $y \in R^n$ denotes the independent time variables and the coordinate vectors of the system, respectively, $\dot{y} \in R^n$, $\ddot{y} \in R^n$ denotes the velocity vector and the acceleration vector of the system, respectively. $\delta \in \sum \subset R^n$ denotes the uncertain parameters of the system, u $\in R^n$ is the control input to the system, and $\hat{M}(y, \delta, t)$, $\hat{Q}(y, \delta, t)$ denotes the mass matrix of the system, respectively, as well as the combined forces of external forces on the system when it is not constrained by the equation. Now let $\hat{M}(\cdot)$ and $\hat{Q}(\cdot)$ denote continuous and measurable with respect to time Lebesgue, then it can be decomposed as shown in equation (7).

$$\begin{cases} \hat{M}(y, \delta, t) = \bar{\hat{M}}(y, t) + \Delta\hat{M}(y, \delta, t) \\ \hat{Q}(y, \delta, t) = \bar{\hat{Q}}(y, t) + \Delta\hat{Q}(y, \delta, t) \end{cases} \tag{7}$$

In equation (7), $\hat{M}$ and $\hat{Q}$ are nominal parts, $\Delta\hat{M}$ and $\Delta\hat{Q}$ are uncertainty parts, and $\bar{\hat{M}}$, $\bar{\hat{Q}}$, $\Delta\bar{\hat{M}}$, $\Delta\bar{\hat{Q}}$ are all continuous as shown in equation (8).

$$\begin{cases} D(y, t) := \bar{\hat{M}}^{-1}(y, t) \\ \Delta D(y, t) := \bar{\hat{M}}^{-1}(y, \delta, t) - \bar{\hat{M}}^{-1}(y, t) \\ E(y, \delta, t) := \bar{\hat{M}}^{-1}(y, t)\bar{\hat{M}}^{-1}(y, \delta, t) - I \end{cases} \tag{8}$$

According to equation (8), $\Delta D(y, \delta, t) := D(y, t)E(y, \delta, t)$. Robust control allows the system to follow the desired trajectory or perform the task stably under these constraints by taking uncertainties into account. By analyzing the uncertainties in the fuzzy description, the stability bounds and performance limits of the system in different situations can be determined [19]. A fuzzy set is a mapping from set X to interval [0, 1] on the domain U of A, as shown in equation (9).

$$A : X \to [0, 1], x \to A(x) \tag{9}$$

In equation (9), A is a fuzzy set on the domain U and $A(x)$ represents the affiliation function on A. Fuzzy sets are a mathematical tool for dealing with uncertainty and ambiguity, they allow elements to have incompletely determined degrees of affiliation rather than strictly belonging or not belonging to a set [20]. Now let the $\alpha-$ truncation set of a fuzzy set G be an explicit set G_α, in which the explicit set contains the elements whose affiliation value of the G set in which U is located is greater than or equal to α. A fuzzy number G is a fuzzy set on the real number domain R, then the real number G is called a fuzzy number when four conditions need to be satisfied, the first one is that G is a regular fuzzy set, the second one is that G is a convex set, the third one is that the bottom set of G must be bounded, and lastly, all the $\alpha-$-truncated sets are closed spaces. Suppose G is a fuzzy set over the domain $U = [0, 2]$ with the expression of the affiliation function shown in equation (10).

$$\mu_G(v) = \begin{cases} v, & 0 \le v \le 1 \\ 2 - v, & 1 \le v \le 2 \end{cases} \tag{10}$$

According to equation (10), the $\alpha-$-intercept set of the number fuzzy set can be obtained, as shown in Figure 3.

As shown in Figure 3, the affiliation function is a key concept in fuzzy set theory, which is used to measure the degree

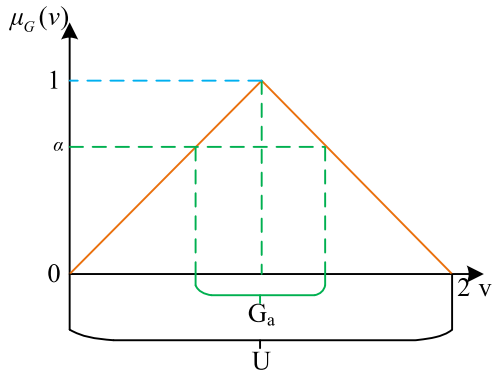

FIGURE 3. Intercept set α of fuzzy set *G*.

of belonging of an element to a fuzzy set [21]. Traditional set theory has only two states, completely belonging or completely not belonging, which cannot describe uncertainty or fuzziness. In contrast, the affiliation function permits a quantitative representation of the relationship between an element and a set, taking values between 0 and 1, with the intermediate value reflecting the degree of ambiguity [22]. Nonlinear time-varying systems integrate nonlinear and time-varying characteristics, the dynamic behaviour does not conform to the principle of linear superposition, and the output-input relationship is complex. The robust control flowchart based on the constraint following theory is shown in Figure 4.

As shown in Figure 4, in control engineering, firstly, the FD model of a mechanical system needs to be established to describe its behaviour in different states, including position, velocity and acceleration [23]. When the model is built, the constraints of the system need to be considered, which can be classified into complete and incomplete structures, and zero-order and first-order constraints according to the order of the constraints. The constraint matrix is used for mathematical representation, which usually requires the consideration of the derivatives of the constraints with respect to time, and sometimes the second order derivatives, especially when describing the acceleration and angular acceleration of the system [24]. Solving problems with constraints usually requires the use of iterative algorithms to find least squares solutions using M-P generalised inverse matrices. Constraint following theory is used to design the CS of a system to ensure that the system satisfies the constraints.

C. FUZZY THEORY FOR DYNAMIC MODELLING IN UMS

The nature of uncertainty lies in the existence of unknown information, which makes the description of the research object lack of certainty and reflects the limited state of knowledge. In the field of engineering, the phenomenon of uncertainty is extremely common, stemming from the existence of numerous unknown factors in the real world, such as environmental changes, the randomness of the nature of the material and so on. The presence of uncertainty has a profound impact on the analysis of the state of a mechanical system and the prediction of future results, as it can trigger changes and uncertainties in the system's behaviour, posing a challenge to the system's performance and stability. Therefore, the consideration and handling of uncertainty must be given high priority in research and engineering practice to ensure the reliability and performance of mechanical systems [25]. The design idea of the safety verification range is shown in Figure 5.

In the design of dynamical models in UMS, control gain is an important parameter that affects the control performance and stability of the system. FC theory provides an effective method for dealing with uncertain systems, which includes the concepts of fuzzy sets and affiliation functions. In FC, the control gain is usually determined by fuzzy reasoning and rule base. In Figure 5, κ_{opt} represents the value of the optimal control gain, $J_1(\kappa, t_s)$ denotes a transient performance metric, which is averaged over the system after the start of time t_s, and this averaging process is achieved by means of the D-operation; $J_2(\kappa)$ reflects the averaged system steady-state performance metrics, and $J_3(\kappa)$ reflects the cost of controlling the whole system.

$$J(\kappa) := h_1 D[\eta_\infty^2(\kappa)] + h_2\kappa^2 =: h_1 J_2(\kappa) + h_2 J_3(\kappa) \quad (11)$$

equation (11) represents the proposed system performance index based on the steady state performance and control cost of the system without considering the constraints of the transient performance of the controlled system.

$$J(W) := h_1 \frac{\lambda_{\max}^2(P)}{4W^2} D[\chi^2] + h_2\kappa^2 =: h_1 \frac{l_4}{\kappa^2} + h^2\kappa^2 \quad (12)$$

Equation (12) represents the optimal design of the control gain κ for the constrained case.

$$\frac{\partial J}{\partial \kappa} = -2h_1 \frac{l_4}{\kappa^2} + 2h_2\kappa = (-2h_1 l_4 + 2h_2\kappa^4)\frac{1}{\kappa^3} \quad (13)$$

Equation (13) represents the rate of change of the calculated performance index with respect to the control gain κ. Let $\frac{\partial J}{\partial \kappa} = 0$, the displacement positive real number solution is shown in equation (14).

$$\kappa_{opt} = \left(\frac{h_1 l_4}{h_2}\right)^{\frac{1}{4}} \quad (14)$$

Due to $D[\chi^2] \neq 0$, $h_1 h_2 > 0$, when the control gain κ has a minimum value, the minimum cost of the system is shown in equation (15).

$$J_{\min} = 2\sqrt{h_1 h_2 l_4} \quad (15)$$

In equation (15), when the weight coefficient $h_1 \to +\infty$, $\kappa_{opt} \to +\infty$, which indicates that the share of control cost associated with that consistent bounded range is elevated, then the associated control gain increases. When the control cost share associated with the uniformly bounded range increases, the corresponding control gain also increases. This is because the weight coefficient in this context represents the control cost share within the consistent bounded range,

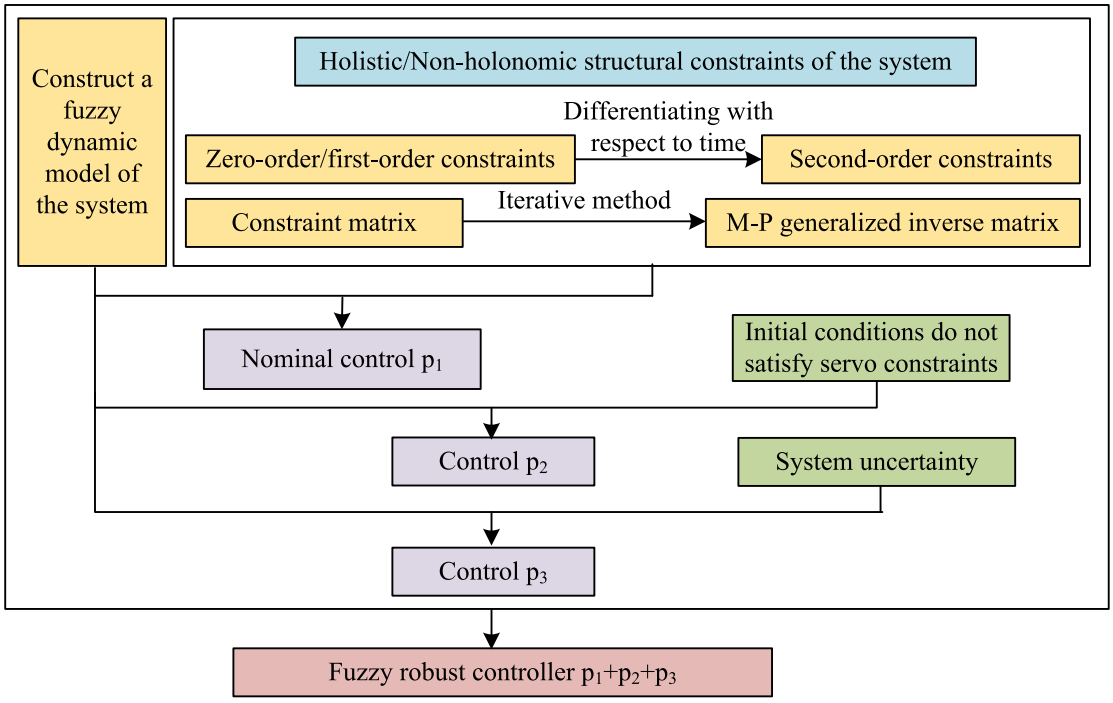

FIGURE 4. Robust control flow chart based on constraint following theory.

and its elevation indicates an increased demand for control within that range. Within the uniformly bounded range, an augmentation of control gain is necessary to better address the dynamic variations and performance requirements of the system. This impact is reflected in the response speed and stability of the system. The increase in control gain enhances the system's ability to regulate its state, thereby accelerating the response speed. However, excessively high control gain may lead to oscillations or unstable behavior in the system. Therefore, the selection of control gain involves a trade-off between response speed and system stability. The choice of control gain is a critical issue in FC because it directly affects the response speed and stability of the system. Usually, the control gain can be adjusted according to the dynamic characteristics and performance requirements of the system. In FC, the control gain is not a definite value but a fuzzy set whose affiliation function can be adjusted according to the change of the system state. The design of control gains needs to take into account the uncertainty and nonlinear characteristics of the system. FC allows the use of fuzzy rules to adjust the control gains to system variations and external perturbations in an uncertain environment. This flexibility gives FC an advantage in dealing with the design of dynamical models for UMS.

IV. FD MODELLING AND CONTROL VALIDATION OF UMS

In this chapter, the control methodology of applying UMS on a permanent magnet synchronous motor will be discussed in detail, and subsequently, the accuracy and applicability of the proposed model will be verified using a designed electrical air throttle. Finally, it is investigated how the control method of UMS can be applied on a permanent magnet synchronous motor.

A. VALIDATION OF THE FD MODEL BUILDING METHOD FOR UMS

FD model construction for UMS is one of the key issues in modern control field, aiming to cope with uncertainties such as parameter variations, external perturbations and modelling errors in order to achieve robust control and high performance operation of the system. The key lies in the introduction of fuzzy set theory to effectively quantify the uncertainty into a subordination function to better understand and deal with the dynamic characteristics of the system. The study will also carry out simulation validation to ensure that the constructed model accurately reflects the performance and robustness of the actual system in the simulation experiments. The parameters of the simulation validation system are shown in Table 1.

According to Table 1, in this mechanical system, the study faces an uncertain external perturbation, denoted by the symbol T_c. Meanwhile, the parameters of the electronic throttle system are as follows: $It = 0.08kgm^2, K_{RD} = 1/360°, K_{DP} = 0.9°/\%, K_{TM} = 0.6, K_{VT} = 0.45, f_v = 40N \cdot m \cdot \min/r, K_{s1} = 0.26Nm/°, K_{s2} = 0.3Nm$. Assuming that the initial condition is $x_0 = [3, -1]$, the study introduces the external perturbation signal $T_c = 2\sin(5t)$ during the simulation. According to the traditional uncertainty treatment, the study can obtain the upper bound of uncertainty as $\bar{e} = 2$. In the simulation, the study considered six different sets of

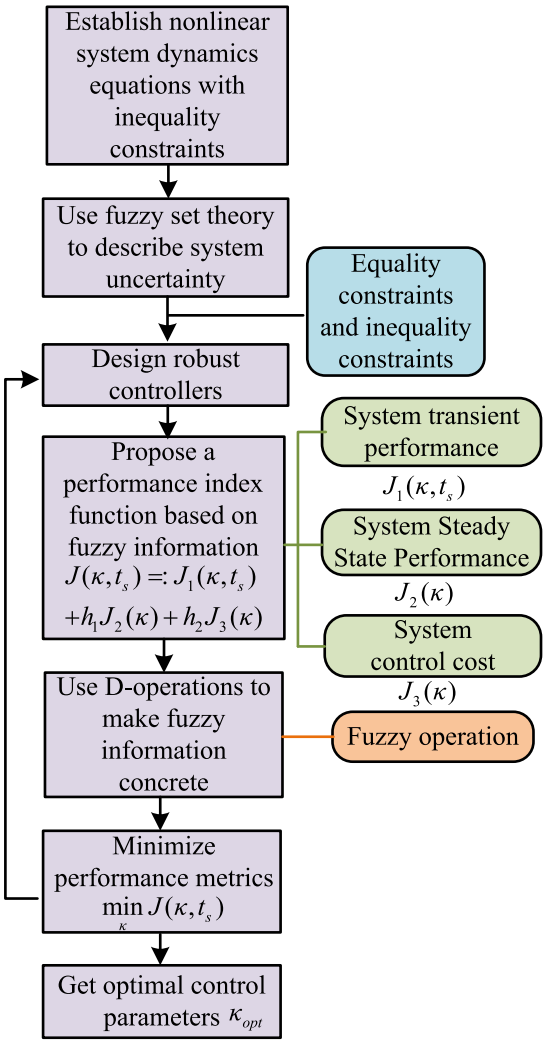

FIGURE 5. Design ideas for safety verification range.

TABLE 1. Simulation verification system parameters.

System parameters	Definition	Unit
θ_v	Relative position of throttle	%/s
$\dot{\theta}_v$	Throttle relative speed	%/s
$\ddot{\theta}_v$	Throttle relative acceleration	%/s2
fv	Viscous friction coefficient	/
It	Concentrated moment of inertia	Kg· m 2
TM	Servo motor torque	N·m
KTM	Gear ratio	/
KVT	Turntable gear ratio	/
KDP	Angle percentage to degree conversion coefficient	°/%
KRD	Angle degrees to radians conversion coefficient	r/°
Ks1	Return spring elastic coefficient	N . m/°
Ks2	Spring bias torque	N·m

λ_1 values (2.05, 2.1, 2.15, 2.2, 2.25, 2.3), and $e = 1$, respectively. To satisfy the assumptions of the study, the study set $\hat{\rho}_1$ to 2.03, 2.08, 2.13, 2.18, 2.23, 2.28, respectively. To simulate the uncertainty of the internal parameters, the study introduced $\Delta I_t = |0.02\cos(3t)|$. The study set the desired trajectory $\theta_d = 15 + 5\sin(2t)$, the desired velocity $\dot{\theta}_d = 10\cos(2t)$, and the desired acceleration $\ddot{\theta}_d = -20\sin(2t)$. Finally, the simulation results show how the control parameters relate to the boundaries and how these parameters limit the size of the control inputs. The CIDA-based control input u1 is shown in Figure 6.

In Figure 6, LQR is a common robust control method that improves system performance by reducing the input gain. The LQR control input gain can be specifically set in the range of 0.2 to 2 to achieve the desired phase difference, typically plus or minus 60 degrees. However, uncertainty in mechanical systems results in excessively large control inputs, increasing the control cost. The CIDA approach compensates for the control inputs by limiting the uncertainty and successfully reduces the control input amplitude by 25 to 40 per cent, reducing the control cost of the system while allowing flexibility in setting the input boundaries based on specific assumptions. The CIDA-based control input U is shown in Figure 7.

Figure 7 demonstrates the comparative results of the total motor inputs, by analysing the total motor input U, the study can understand the effect of the CIDA method in control more comprehensively. According to the dynamical equations of the system, the total motor input U consists of two components, u1 and u2, where u1 is affected by the CIDACS, while the amplitude of u2 is already determined and is not affected by the uncertainty. When using the conventional LQR control method, the amplitude of the total input U to the motor averages about 100 volts, however, when CIDACS is used, the amplitude of u1 is reduced by an average of about 40 volts, which reduces the total input U to an average of about 60 volts, and it can be seen that this control method effectively reduces the total input U of the motor to make it more stable with respect to the situation when using the conventional LQR control method. The CIDA based input maximum and cumulative control inputs are shown in Figure 8.

In Figure 8(a), the maximum value of the bounded part u1 is demonstrated for different control inputs. The observations strongly support the CIDA method by showing that the maximum value of u1 is controlled by the upper bound limit, further validating the effectiveness of the method. This effective control input amplitude maintains the stability of the system, which is crucial for the controllability of the UMS. By keeping the control input fluctuating within an acceptable range, the CIDA method is expected to improve the robustness of the system. In Figure 8(b), the study also explores the comparison of cumulative control inputs of the motor. By analysing the comparison, it is clearly visible that the cumulative control input of the motor is significantly less with the CIDA method than with the conventional LQR control method. The system location of CIDA is shown in Figure 9.

Figure 9 shows the comparison of the position tracking performance of the system under different control methods.

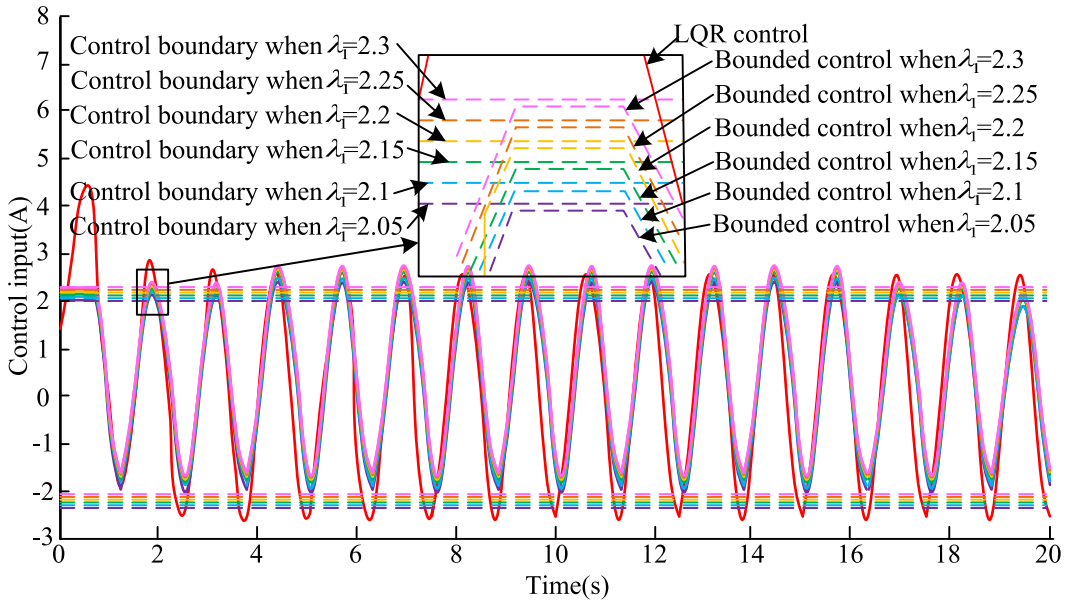

FIGURE 6. CIDA-based control input u_1.

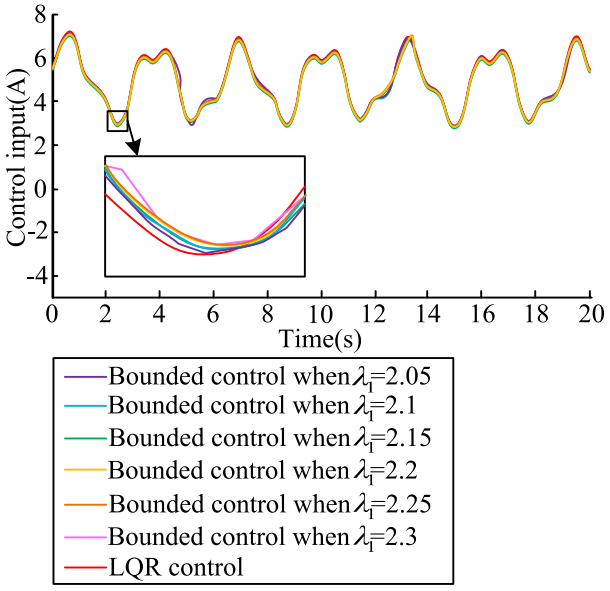

FIGURE 7. CIDA-based control input U.

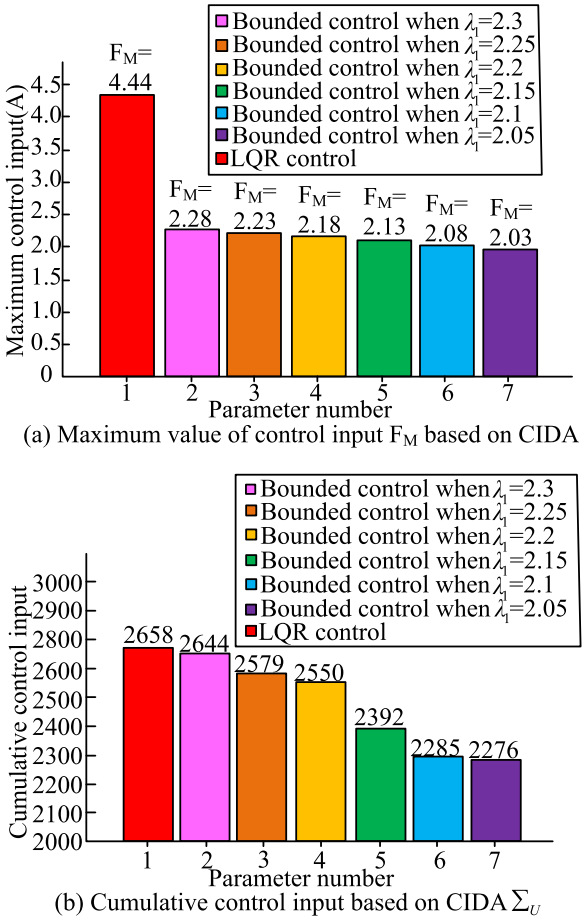

FIGURE 8. CIDA-based input maximum value and cumulative control input.

Under CIDA control, the position tracking ability of the system is very strong and the average position error of the system can be maintained at about 1 mm. On the other hand, the input limits of the system change under different boundary values. When the control boundary value is small, the control input range of the system is limited and averages around 80 volts. As the boundary value increases to 120 volts, the average control input range of the system can be extended to 110 volts. The system speed of CIDA is shown in Figure 10.

Figure 10 demonstrates a comparison of the change in system angle under different control methods. Under CIDA control, the system angle tracking shows excellent stability and accuracy. This implies that the CIDA method can effectively cope with the angular control problem in UMS and

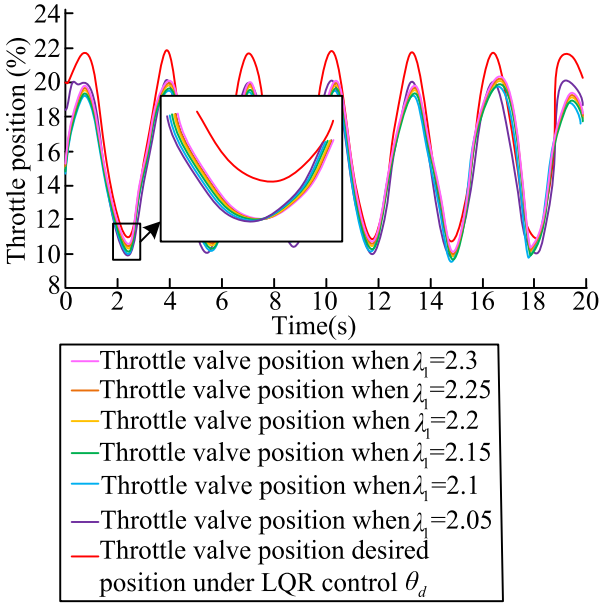

FIGURE 9. CIDA based system location θ_v.

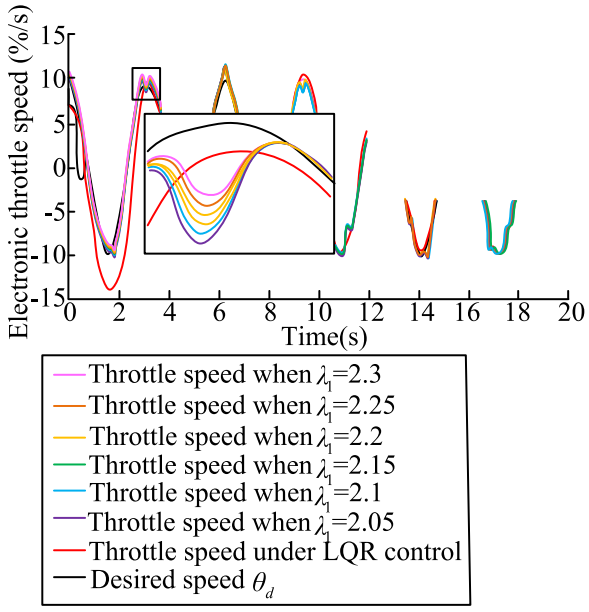

FIGURE 10. CIDA-based system speed θ_v.

ensure that the system angle can closely track the desired trajectory. It is particularly noteworthy that the input range of the system changes at different boundary values. As the boundaries increase, the system obtains a larger control input magnitude, which leads to an improvement in the angular tracking performance of the system. This means that the CIDA method allows the control boundaries to be adjusted according to the actual needs for more flexible control and thus better meets the performance requirements of the UMS. The cumulative output error of the system for CIDA is shown in Figure 11.

Figure 11 demonstrates the cumulative output error of the system, which is one of the key metrics for evaluating the

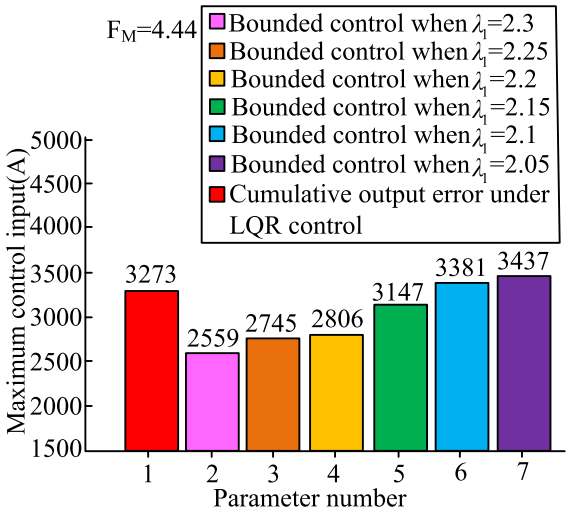

FIGURE 11. Cumulative output error of system based on CIDA $\sum_x$.

performance of the UMS. Comparing the cumulative output error under different control methods highlights the performance improvement effect of the CIDA method. Firstly, it can be observed that the CIDA method significantly reduces the cumulative output error and improves the tracking performance of the system, which is crucial for the UMS because the accumulation of output error may impair the system performance. Secondly, the system performance gradually improves as the boundary increases, indicating that the CIDA method allows flexibility in adjusting the boundary values according to different performance requirements. Increasing the boundary provides a larger input amplitude and reduces the output error, thus improving the tracking accuracy of the system.

B. VALIDATION OF UMS CONTROL METHOD ON PMSM

The core of the experimental equipment is a TMS320F28335 Digital Signal Processing Controller (DSP), which controls the Permanent Magnet Synchronous Motor (PMSM) system and is responsible for data acquisition. Matlab/Simulink is used on the PC to construct the mathematical model and to generate the code for the control algorithm. Another PMSM is introduced in the experiment to simulate the external perturbation by random current. The whole experimental platform includes two PMSMs, torque transducers and couplings, and the desired trajectory is defined as $\theta_d = 2\pi \sin(0.2t)$. The State-Dependent Control Approach (STA)-based, Robust Control Approach (HORC)-based, Optimisation-Based Approach (GTOA) are shown in Figure 12.

The trajectories of the PMSM turn angle in different cases, including the upper and lower bounds (6m and 0m) as well as the desired trajectory, are presented in Figure 12. The figure is analysed in detail as follows, firstly, it shows that the trajectories of the four different experiments can effectively track the desired trajectory, and the average angular

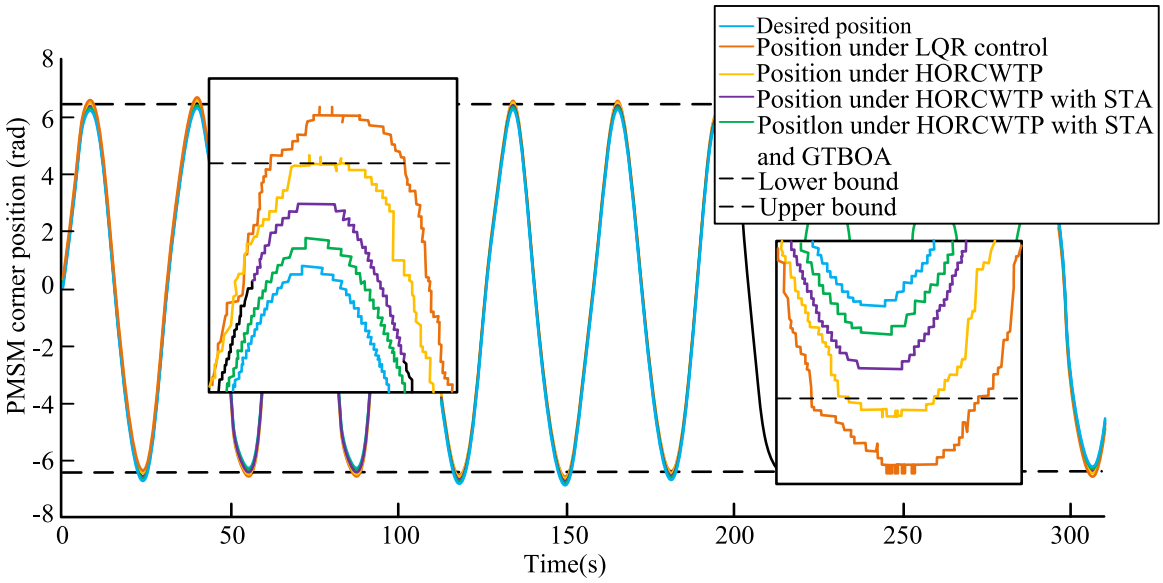

FIGURE 12. Position θ_p based on STA, HORC, GTOA.

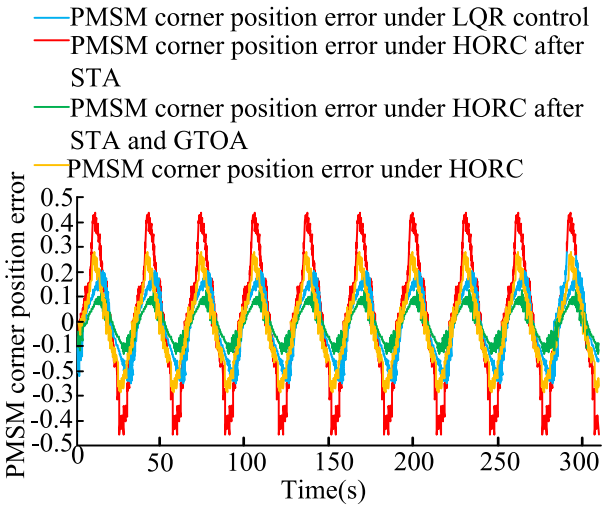

FIGURE 13. Error based on STA, HORC, GTOA e_p.

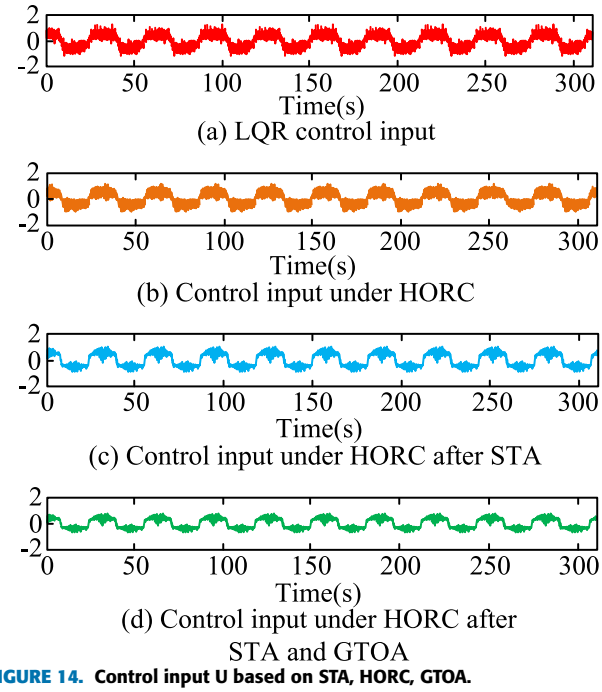

FIGURE 14. Control input U based on STA, HORC, GTOA.

errors of experiments A,B,C,D are about 0.5 degree, 1 degree, 0.3 degree and 0.8 degree respectively, which shows that the trajectory of experiment A is the closest to the desired trajectory. Secondly, the trajectories in both Experiments A and B exceeded the upper bound, and the control input amplitude averaged within 7.5m and 8m in Experiments A and B, respectively. In contrast, the trajectories in both Experiments C and D stayed within the upper and lower bounds, with the control input amplitude averaging within 4.5m in Experiment C, and within 3m in Experiment D using the optimal GTOA-based control parameters. Finally, the figure also clearly demonstrates that the STA method is able to better suppress random external disturbances when the trajectories are close to the extremes, and the angular errors of experiment D are within 0.6 degrees on average when the trajectories are close to the extremes, while the angular errors of experiment C are within 1.5 degrees on average. The errors based on STA, HORC, and GTOA are shown in Figure 13.

Figure 13 presents the performance of the systematic error in different cases, and it is noteworthy that the error in Experiment D reaches the minimum value. This means that the HORCCS combining STA and GTOA exhibits the most excellent control in the study. Secondly, the HORC control with STA also showed a decent performance in terms of

error, although slightly inferior to the combination of STA and GTOA. Finally, the results of the standalone application of HORCCS are also considerable, although slightly inferior to the first two. The control input U based on STA, HORC, and GTOA is shown in Figure 14.

The evolution curves of the control inputs over time for different cases are shown in Figure 14. Observing these curves, the study can draw some important conclusions. Firstly, under HORCCS, the peak value of the control input is significantly reduced compared to the conventional LQR control, while the curve is smoother. This indicates that HORCCS can effectively reduce the peak value of the control input of the motor system, which reduces the energy consumption and mechanical wear of the system and improves the stability and efficiency of the system. Secondly, the standard deviation of the current fluctuation is reduced by 10% on average after the introduction of the STA method.

V. CONCLUSION

In contemporary society, mechanical systems are indispensable across a diverse array of industries, from an automated production line to a transport system or a medical device. The performance and reliability of these systems are critical in maintaining seamless business operations and sustaining human life. To this end, research primarily concentrates on efficaciously managing constraints to guarantee system stability. Secondly, these techniques utilise robust control theory for examining system performance and stability, with specific attention to constraints. Lastly, they implement fuzzy theory to develop more precise dynamics to enhance comprehending system behaviour and managing uncertainties. The study findings demonstrated that LQR control techniques generally establish the input gain range between 0.2 to 2 to attain a phase difference of plus or minus 60 degrees in control. Nevertheless, due to the uncertainties in mechanical systems, the average control input was about 100 volts, contributing to an increased control cost. To address this issue, the CIDA approach successfully decreased the amplitude of control input by 25-40%, resulting in an average total input U of approximately 60 volts and significant enhancement of the system's stability. Additionally, regarding overall motor input, the amplitude of u1 decreased by approximately 40 volts on average with the implementation of the CIDA strategy. Simultaneously, the average position error remained at roughly 1 mm with CIDA. Furthermore, the system's control input range varied under various boundary conditions, with an average of approximately 80 volts for smaller boundary values, yet it could be extended to an average of 110 volts with an increase of the boundary value to 120 volts. In the cornering trajectory experiments of PMSMs, all trials successfully followed the desired paths with an average angular error of approximately 0.5, 1, 0.3, and 0.8 degrees for Experiments A, B, C, and D respectively. Notably, Experiments A and B surpassed the upper limit in some instances while Experiments C and D remained within both upper and lower bounds. Finally, in relation to control inputs, the implementation of HORCCS exhibited a considerable decrease in peaks, reducing them from approximately 140 volts in conventional LQR control to around 100 volts, with a smoother curve. With the introduction of the STA method, the standard deviation of current fluctuations decreased by an average of 10%. This method further enhances the stability and efficiency of the motor system. The data and observations indicate that the implementation of CIDA, HORC, and STA strategies resulted in a significant improvement of mechanical system performance and stability. The precision control strategy based on fuzzy dynamics involves the introduction of a fuzzy logic system to model the dynamics of uncertain mechanical systems. Fuzzy theory allows for flexible handling of system nonlinearity and uncertainty, providing a more accurate description of system behavior. In the control strategy, the fuzzy dynamics model can adapt to dynamic changes and external disturbances, enhancing the robustness and adaptability of the system. Secondly, robust control theory is utilized to evaluate the system's performance and stability under constrained conditions. The introduction of the constraint-invariant dynamic analysis method reduces control input amplitudes, effectively improving system stability. Through robust control, the study can analyze the system's response under specific constraint conditions, ensuring the system maintains good performance under constraints. However, the study's limitations suggest that the applicability of the methods is contingent upon specific circumstances, and more flexible approaches are necessary to address extensive and complex uncertainty situations.

REFERENCES

[1] H. Huang, H. Weng, and J. Chen, "The biogenesis and precise control of RNA m6A methylation," *Trends Genet.*, vol. 36, no. 1, pp. 44–52, Jan. 2020, doi: 10.1016/j.tig.2019.10.011.

[2] Y. Yin, B. Luo, H. Ren, Q. Fang, and C. Zhang, "Robust control design for active suspension system with uncertain dynamics and actuator time delay," *J. Mech. Sci. Technol.*, vol. 36, no. 12, pp. 6319–6327, Dec. 2022, doi: 10.1007/s12206-022-1143-1.

[3] W. Ji, J. Qiu, L. Wu, and H.-K. Lam, "Fuzzy-affine-model-based output feedback dynamic sliding mode controller design of nonlinear systems," *IEEE Trans. Syst. Man, Cybern. Syst.*, vol. 51, no. 3, pp. 1652–1661, Mar. 2021, doi: 10.1109/TSMC.2019.2900050.

[4] W. S. Cortez, D. Oetomo, C. Manzie, and P. Choong, "Control barrier functions for mechanical systems: Theory and application to robotic grasping," *IEEE Trans. Control Syst. Technol.*, vol. 29, no. 2, pp. 530–545, Mar. 2021, doi: 10.1109/TCST.2019.2952317.

[5] T. Yang, N. Sun, and Y. Fang, "Adaptive fuzzy control for a class of MIMO underactuated systems with plant uncertainties and actuator deadzones: Design and experiments," *IEEE Trans. Cybern.*, vol. 52, no. 8, pp. 8213–8226, Aug. 2022, doi: 10.1109/TCYB.2021.3050475.

[6] Z. Zhao, C. K. Ahn, and H.-X. Li, "Dead zone compensation and adaptive vibration control of uncertain spatial flexible riser systems," *IEEE/ASME Trans. Mechatronics*, vol. 25, no. 3, pp. 1398–1408, Jun. 2020, doi: 10.1109/TMECH.2020.2975567.

[7] J. Liu, M. Yang, X. Xie, C. Peng, and H. Yan, "Finite-time H_∞ filtering for state-dependent uncertain systems with event-triggered mechanism and multiple attacks," *IEEE Trans. Circuits Syst. I, Reg. Papers*, vol. 67, no. 3, pp. 1021–1034, Mar. 2020, doi: 10.1109/TCSI.2019.2949014.

[8] J. Liu, M. Yang, E. Tian, J. Cao, and S. Fei, "Event-based security control for state-dependent uncertain systems under hybrid-attacks and its application to electronic circuits," *IEEE Trans. Circuits Syst. I, Reg. Papers*, vol. 66, no. 12, pp. 4817–4828, Dec. 2019, doi: 10.1109/TCSI.2019.2930572.

[9] W. Ji, J. Qiu, and H. R. Karimi, "Fuzzy-model-based output feedback sliding-mode control for discrete-time uncertain nonlinear systems," *IEEE Trans. Fuzzy Syst.*, vol. 28, no. 8, pp. 1519–1530, Aug. 2020, doi: 10.1109/TFUZZ.2019.2917127.
[10] H. Huang, C. Yang, and C. L. P. Chen, "Optimal robot–environment interaction under broad fuzzy neural adaptive control," *IEEE Trans. Cybern.*, vol. 51, no. 7, pp. 3824–3835, Jul. 2021, doi: 10.1109/TCYB.2020.2998984.
[11] X. Liang, X. Qu, N. Wang, R. Zhang, and Y. Li, "Three-dimensional trajectory tracking of an underactuated AUV based on fuzzy dynamic surface control," *IET Intell. Transp. Syst.*, vol. 14, no. 5, pp. 364–370, Nov. 2019, doi: 10.1049/iet-its.2019.0347.
[12] X. Wang, L. Lei, L. Wang, P. Yang, and H. Chen, "Spatial colocation pattern discovery incorporating fuzzy theory," *IEEE Trans. Fuzzy Syst.*, vol. 30, no. 6, pp. 2055–2072, Jun. 2022, doi: 10.1109/TFUZZ.2021.3074074.
[13] Y. Hu, L. Wu, X. Pan, Z. Wang, and X. Xu, "Comprehensive evaluation of cloud manufacturing service based on fuzzy theory," *Int. J. Fuzzy Syst.*, vol. 23, no. 6, pp. 1755–1764, May 2021, doi: 10.1007/s40815-021-01071-4.
[14] B. Hanin, "Universal function approximation by deep neural nets with bounded width and ReLU activations," *Mathematics*, vol. 7, no. 10, p. 992, Oct. 2019, doi: 10.3390/math7100992.
[15] H. K. Matthews, C. Bertoli, and R. A. M. de Bruin, "Cell cycle control in cancer," *Nature Rev. Mol. Cell Biol.*, vol. 23, no. 1, pp. 74–88, Jan. 2022, doi: 10.1038/s41580-021-00404-3.
[16] Y. Hu, H. Wang, S. He, J. Zheng, Z. Ping, K. Shao, Z. Cao, and Z. Man, "Adaptive tracking control of an electronic throttle valve based on recursive terminal sliding mode," *IEEE Trans. Veh. Technol.*, vol. 70, no. 1, pp. 251–262, Jan. 2021, doi: 10.1109/TVT.2020.3045778.
[17] L. Gao, J. Yuan, and Y. Qian, "Torque control based direct teaching for industrial robot considering temperature-load effects on joint friction," *Ind. Robot, Int. J. Robot. Res. Appl.*, vol. 46, no. 5, pp. 699–710, Aug. 2019, doi: 10.1108/IR-12-2018-0254.
[18] H. Li, G. Li, Q. Wang, B. Ju, and Y. Wen, "Friction torque field distribution of a permanent-magnet spherical motor based on multi-physical field coupling analysis," *IET Electr. Power Appl.*, vol. 15, no. 8, pp. 1045–1055, Jun. 2021, doi: 10.1049/elp2.12096.
[19] G. Duan, "High-order fully actuated system approaches: Part III. Robust control and high-order backstepping," *Int. J. Syst. Sci.*, vol. 52, no. 5, pp. 952–971, Apr. 2021, doi: 10.1080/00207721.2020.1849863.
[20] Z. Wang, A. Yu, X. Li, G. Zhang, and C. Xia, "A novel current predictive control based on fuzzy algorithm for PMSM," *IEEE J. Emerg. Sel. Topics Power Electron.*, vol. 7, no. 2, pp. 990–1001, Jun. 2019, doi: 10.1109/JESTPE.2019.2902634.
[21] Z. Yuan, C. Jin, and Z. Chen, "Research on language analysis of English translation system based on fuzzy algorithm," *J. Intell. Fuzzy Syst.*, vol. 40, no. 4, pp. 6039–6047, Apr. 2021, doi: 10.3233/JIFS-189443.
[22] S. Liu, S. Wang, X. Liu, C.-T. Lin, and Z. Lv, "Fuzzy detection aided real-time and robust visual tracking under complex environments," *IEEE Trans. Fuzzy Syst.*, vol. 29, no. 1, pp. 90–102, Jan. 2021, doi: 10.1109/TFUZZ.2020.3006520.
[23] N. Priyadarshi, S. Padmanaban, J. B. Holm-Nielsen, F. Blaabjerg, and M. S. Bhaskar, "An experimental estimation of hybrid ANFIS–PSO-based MPPT for PV grid integration under fluctuating sun irradiance," *IEEE Syst. J.*, vol. 14, no. 1, pp. 1218–1229, Mar. 2020, doi: 10.1109/JSYST.2019.2949083.
[24] Y. Saidi, A. Nemra, and M. Tadjine, "Robust mobile robot navigation using fuzzy type 2 with wheel slip dynamic modeling and parameters uncertainties," *Int. J. Model. Simul.*, vol. 40, no. 6, pp. 397–420, Nov. 2020, doi: 10.1080/02286203.2019.1646480.
[25] J. Li, J. Wang, H. Peng, Y. Hu, and H. Su, "Fuzzy-torque approximation-enhanced sliding mode control for lateral stability of mobile robot," *IEEE Trans. Syst. Man, Cybern. Syst.*, vol. 52, no. 4, pp. 2491–2500, Apr. 2022, doi: 10.1109/TSMC.2021.3050616.
[26] M. R. Khan, K. Ullah, D. Dragan Pamucar, and M. Bari, "Performance measure using a multi-attribute decision-making approach based on complex T-spherical fuzzy power aggregation operators," *J. Comput. Cognit. Eng.*, vol. 1, no. 3, pp. 138–146, Feb. 2022, doi: 10.47852/bonviewJCCE696205514.

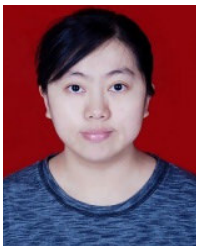

CHENDI SHI was born in Siping, Jilin, China, in January 1983. She received the bachelor's degree in computer science and technology from the Changchun University of Science and Technology, in 2006, and the master's degree in computer technology from the Changchun University of Science and Technology, in 2012, with a research direction in mechanical design and manufacturing.

From 2006 to 2021, she was a Teacher with the Department of Mechanical and Electrical Engineering, Jilin Engineering Vocational College, where she has been the Vice Dean with the Department of Rural Revitalization Education, since 2021. Her academic works, include 23 academic papers, three academic works, and textbooks. She has published 22 scientific research projects and eight patents and received 52 academic awards.

BAO LIU was born in Siping, Jilin, China, in March 1982. He received the bachelor's degree in accounting from the Jilin Province Economic Management Cadre College, in 2015, with a research direction in accounting.

He was an Office Clerk (1999–2014) and a Finance Department Clerk (2014–2018) with the Jilin Engineering Vocational College, where he has been an Experimenter with the Department of Management, since 2018. He has published two academic papers, 11 scientific research projects, and two patents.